

1 **A GENERALISED RANDOM ENCOUNTER MODEL FOR ESTIMATING**
2 **ANIMAL DENSITY WITH REMOTE SENSOR DATA**

3 **Running title: A generalised random encounter model for animals.**

4 **Word count:** 7158

5 **Authors:**

6 Tim C.D. Lucas^{1,2,3,†}, Elizabeth A. Moorcroft^{1,4,5,†}, Robin Freeman⁵, Marcus J. Rowcliffe⁵,
7 Kate E. Jones^{2,5}

8 **Addresses:**

9 1 CoMPLEX, University College London, Physics Building, Gower Street, Lon-
10 don, WC1E 6BT, UK

11 2 Centre for Biodiversity and Environment Research, Department of Genetics,
12 Evolution and Environment, University College London, Gower Street, London,
13 WC1E 6BT, UK

14 3 Department of Statistical Science, University College London, Gower Street,
15 London, WC1E 6BT, UK

16 4 Department of Computer Science, University College London, Gower Street,
17 London, WC1E 6BT, UK

18 5 Institute of Zoology, Zoological Society of London, Regents Park, London, NW1
19 4RY, UK

20 † First authorship shared.

21 **Corresponding authors:**

22 Kate E. Jones,
23 Centre for Biodiversity and Environment Research,
24 Department of Genetics, Evolution and Environment,
25 University College London,
26 Gower Street,
27 London,
28 WC1E 6BT,

29 UK

30 kate.e.jones@ucl.ac.uk

31

32 Marcus J. Rowcliffe,

33 Institute of Zoology,

34 Zoological Society of London,

35 Regents Park,

36 London,

37 NW1 4RY,

38 UK

39 marcus.rowcliffe@ioz.ac.uk

ABSTRACT

40
41 **1:** Wildlife monitoring technology is advancing rapidly and the use of remote sen-
42 sors such as camera traps and acoustic detectors is becoming common in both the
43 terrestrial and marine environments. Current methods to estimate abundance or
44 density require individual recognition of animals or knowing the distance of the
45 animal from the sensor, which is often difficult. A method without these require-
46 ments, the random encounter model (REM), has been successfully applied to es-
47 timate animal densities from count data generated from camera traps. However,
48 count data from acoustic detectors do not fit the assumptions of the REM due to
49 the directionality of animal signals.

50 **2:** We developed a generalised REM (gREM), to estimate absolute animal density
51 from count data from both camera traps and acoustic detectors. We derived the
52 gREM for different combinations of sensor detection widths and animal signal
53 widths (a measure of directionality). We tested the accuracy and precision of this
54 model using simulations of different combinations of sensor detection widths and
55 animal signal widths, number of captures, and models of animal movement.

56 **3:** We find that the gREM produces accurate estimates of absolute animal density
57 for all combinations of sensor detection widths and animal signal widths. How-
58 ever, larger sensor detection and animal signal widths were found to be more pre-
59 cise. While the model is accurate for all capture efforts tested, the precision of the
60 estimate increases with the number of captures. We found no effect of different
61 animal movement models on the accuracy and precision of the gREM.

62 **4:** We conclude that the gREM provides an effective method to estimate absolute
63 animal densities from remote sensor count data over a range of sensor and animal
64 signal widths. The gREM is applicable for count data obtained in both marine
65 and terrestrial environments, visually or acoustically (e.g., big cats, sharks, birds,
66 echolocating bats and cetaceans). As sensors such as camera traps and acous-
67 tic detectors become more ubiquitous, the gREM will be increasingly useful for
68 monitoring unmarked animal populations across broad spatial, temporal and tax-
69 onomic scales.

70 **Keywords.** Acoustic detection, camera traps, marine, population monitoring, sim-
71 ulations, terrestrial

72 INTRODUCTION

73 The density of animal populations is one of the fundamental measures in ecol-
74 ogy and conservation and has important implications for a range of issues, such
75 as sensitivity to stochastic fluctuations (Wright & Hubbell, 1983) and extinction
76 risk (Purvis *et al.*, 2000). Monitoring animal population changes in response to
77 anthropogenic pressure is becoming increasingly important as humans rapidly
78 modify habitats and change climates (Everatt *et al.*, 2014). Sensor technology, such
79 as camera traps (Karanth, 1995; Rowcliffe & Carbone, 2008) and acoustic detec-
80 tors (Acevedo & Villanueva-Rivera, 2006; Walters *et al.*, 2012) are widely used to
81 monitor changes in animal populations as they are efficient, relatively cheap and
82 non-invasive, allowing for surveys over large areas and long periods (Rowcliffe &
83 Carbone, 2008; Kessel *et al.*, 2014; Walters *et al.*, 2013). However, converting sam-
84 pled count data into estimates of density is problematic as detectability of animals
85 needs to be accounted for (Anderson, 2001).

86 Existing methods for estimating animal density often require additional infor-
87 mation that is often unavailable. For example, capture-mark-recapture methods
88 (Karanth, 1995; Borchers *et al.*, 2014) require recognition of individuals, and dis-
89 tance methods (Harris *et al.*, 2013) require estimates of how far away individuals
90 are from the sensor (Barlow & Taylor, 2005; Marques *et al.*, 2011). When individ-
91 uals cannot be told apart, an extension of occupancy modelling can be used to
92 estimate absolute abundance (Royle & Nichols, 2003). However, as the model is
93 originally formulated to estimate occupancy, count information is simplified to
94 presence-absence data. Assumptions about the distribution of individuals (e.g. a
95 poisson distribution) must also be made (Royle & Nichols, 2003) which may be a
96 poor assumption for nonrandomly distributed species. Furthermore repeat, inde-
97 pendent surveys must be performed and the definition of a site can be difficult,
98 especially for wide-ranging species (MacKenzie & Royle, 2005).

99 More recently, the development of the random encounter model (REM), a mod-
 100 ification of an ideal gas model (Yapp, 1956; Hutchinson & Waser, 2007), has en-
 101 abled animal densities to be estimated from unmarked individuals of a known
 102 speed, and with known sensor detection parameters (Rowcliffe *et al.*, 2008). The
 103 REM method has been successfully applied to estimate animal densities from cam-
 104 era trap surveys (Zero *et al.*, 2013). However, extending the REM method to other
 105 types of sensors (e.g., acoustic detectors) is more problematic, because the original
 106 derivation assumes a relatively narrow sensor width (up to $\pi/2$ radians) and that
 107 the animal is equally detectable irrespective of its heading (Rowcliffe *et al.*, 2008).

108 Whilst these restrictions are not problematic for most camera trap makes (e.g.,
 109 Reconyx, Cuddeback), the REM cannot be used to estimate densities from camera
 110 traps with a wider sensor width (e.g. canopy monitoring with fish eye lenses,
 111 Brusa & Bunker (2014)). Additionally, the REM method is not useful in estimating
 112 densities from acoustic survey data as acoustic detector angles are often wider
 113 than $\pi/2$ radians. Acoustic detectors are designed for a range of diverse tasks
 114 and environments (Kessel *et al.*, 2014), which naturally leads to a wide range of
 115 sensor detection widths and detection distances. In addition to this, calls emitted
 116 by many animals are directional (Blumstein *et al.*, 2011), breaking the assumption
 117 of the REM method.

118 There has been a sharp rise in interest around passive acoustic detectors in re-
 119 cent years, with a 10 fold increase in publications in the decade between 2000 and
 120 2010 (Kessel *et al.*, 2014). Acoustic monitoring is being developed to study many
 121 aspects of ecology, including the interactions of animals and their environments
 122 (Blumstein *et al.*, 2011; Rogers *et al.*, 2013), the presence and relative abundances of
 123 species (Marcoux *et al.*, 2011), biodiversity of an area (Depraetere *et al.*, 2012), and
 124 monitoring population trends (Walters *et al.*, 2013).

125 Acoustic data suffers from many of the problems associated with data from
 126 camera trap surveys in that individuals are often unmarked, making capture-
 127 mark-recapture methods more difficult to use (Marques *et al.*, 2013). In some cases
 128 the distance between the animal and the sensor is known, for example when an
 129 array of sensors is deployed and the position of the animal is estimated by trian-
 130 gulation (Lewis *et al.*, 2007). In these situations distance-sampling methods can be

131 applied, a method typically used for marine mammals (Rogers *et al.*, 2013). How-
 132 ever, in many cases distance estimation is not possible, for example when single
 133 sensors are deployed, a situation typical in the majority of terrestrial acoustic sur-
 134 veys (Buckland *et al.*, 2008). In these cases, only relative measures of local abun-
 135 dance can be calculated, and not absolute densities. This means that comparison
 136 of populations between species and sites is problematic without assuming equal
 137 detectability (Schmidt, 2003; Walters *et al.*, 2013). Equal detectability is unlikely be-
 138 cause of differences in environmental conditions, sensor type, habitat, and species
 139 biology.

140 In this study, we create a generalised REM (gREM) as an extension to the cam-
 141 era trap model of Rowcliffe *et al.* (2008), to estimate absolute density from count
 142 data from acoustic detectors, or camera traps, where the sensor width can vary
 143 from 0 to 2π radians, and the signal given from the animal can be directional. We
 144 assessed the accuracy and precision of the gREM within a simulated environment,
 145 by varying the sensor detection widths, animal signal widths, number of captures
 146 and models of animal movement. We use the simulation results to recommend
 147 best survey practice for estimating animal densities from remote sensors.

148 METHODS

149 **Analytical Model.** The REM presented by Rowcliffe *et al.* (2008) adapts the gas
 150 model to count data collected from camera trap surveys. The REM is derived
 151 assuming a stationary sensor with a detection width less than $\pi/2$ radians. How-
 152 ever, in order to apply this approach more generally, and in particular to stationary
 153 acoustic detectors, we need both to relax the constraint on sensor detection width,
 154 and allow for animals with directional signals. Consequently, we derive the gREM
 155 for any detection width, θ , between 0 and 2π with a detection distance r giving a
 156 circular sector within which animals can be captured (the detection zone) (Fig-
 157 ure 1). Additionally, we model the animal as having an associated signal width
 158 α between 0 and 2π (Figure 1, see Appendix S1 for a list of symbols). We start
 159 deriving the gREM with the simplest situation, the gas model where $\theta = 2\pi$ and
 160 $\alpha = 2\pi$.

161 *Gas Model.* Following Yapp (1956), we derive the gas model where sensors can
 162 capture animals in any direction and animal signals are detectable from any direc-
 163 tion ($\theta = 2\pi$ and $\alpha = 2\pi$). We assume that animals are in a homogeneous environ-
 164 ment, and move in straight lines of random direction with velocity v . We allow
 165 that our stationary sensor can capture animals at a detection distance r and that if
 166 an animal moves within this detection zone they are captured with a probability
 167 of one; while outside this zone, animals are never captured.

168 In order to derive animal density, we need to consider relative velocity from the
 169 reference frame of the animals. Conceptually, this requires us to imagine that all
 170 animals are stationary and randomly distributed in space, while the sensor moves
 171 with velocity v . If we calculate the area covered by the sensor during the survey
 172 period, we can estimate the number of animals the sensor should capture. As a
 173 circle moving across a plane, the area covered by the sensor per unit time is $2rv$.
 174 The expected number of captures, z , for a survey period of t , with an animal den-
 175 sity of D is $z = 2rvtD$. To estimate the density we rearrange to get $D = z/2rvt$. Note
 176 that as z is the number of encounters, not individuals, the possibility of repeated
 177 detections of the same individual is accounted for (Hutchinson & Waser, 2007).

178 *gREM derivations for different detection and signal widths.* Different combinations of
 179 θ and α would be expected to occur (e.g., sensors have different detection widths
 180 and animals have different signal widths). For different combinations θ and α , the
 181 area covered per unit time is no longer given by $2rv$. Instead of the size of the
 182 sensor detection zone having a diameter of $2r$, the size changes with the approach
 183 angle between the sensor and the animal. The width of the area within which an
 184 animal can be detected is called the profile, p . The size of p depends on the signal
 185 width, detector width and the angle that the animal approaches the sensor. The
 186 size of the profile (averaged across all approach angles) is defined as the average
 187 profile \bar{p} . However, different combinations of θ and α need different equations to
 188 calculate \bar{p} .

189 We have identified the parameter space for the combinations of θ and α for
 190 which the derivation of the equations are the same (defined as sub-models in the

gREM) (Figure 2). For example, the gas model becomes the simplest gREM sub-model (upper right in Figure 2) and the REM from Rowcliffe *et al.* (2008) is another gREM sub-model where $\theta < \pi/2$ and $\alpha = 2\pi$. We derive one gREM sub-model SE2 as an example below, where $2\pi - \alpha/2 < \theta < 2\pi$, $0 < \alpha < \pi$ (see Appendix S2 for derivations of all gREM sub-models). Any estimate of density would require prior knowledge of animal velocity, v and animal signal width, α taken from other sources, for example existing literature (Brinkløv *et al.*, 2011; Carbone *et al.*, 2005). Sensor width, θ , and detection distance, r would also need to be measured or obtained from manufacturer specifications (Holderied & Von Helversen, 2003; Adams *et al.*, 2012).

Example derivation of SE2. In order to calculate \bar{p} , we have to integrate over the focal angle, x_1 (Figure 3a). This is the angle taken from the centre line of the sensor. Other focal angles are possible (x_2, x_3, x_4) and are used in other gREM sub-models (see Appendix S2). As the size of the profile depends on the approach angle, we present the derivation across all approach angles. When the sensor is directly approaching the animal $x_1 = \pi/2$.

Starting from $x_1 = \pi/2$ until $\theta/2 + \pi/2 - \alpha/2$, the size of the profile is $2r \sin \alpha/2$ (Figure 3b). During this first interval, the size of α limits the width of the profile. When the animal reaches $x_1 = \theta/2 + \pi/2 - \alpha/2$ (Figure 3c), the size of the profile is $r \sin(\alpha/2) + r \cos(x_1 - \theta/2)$ and the size of θ and α both limit the width of the profile (Figure 3c). Finally, at $x_1 = 5\pi/2 - \theta/2 - \alpha/2$ until $x_1 = 3\pi/2$, the width of the profile is again $2r \sin \alpha/2$ (Figure 3d) and the size of α again limits the width of the profile.

The profile width p for π radians of rotation (from directly towards the sensor to directly behind the sensor) is completely characterised by the three intervals (Figure 3b–d). Average profile width \bar{p} is calculated by integrating these profiles over their appropriate intervals of x_1 and dividing by π which gives

$$\bar{p} = \frac{1}{\pi} \left(\int_{\frac{\pi}{2}}^{\frac{\pi}{2} + \frac{\theta}{2} - \frac{\alpha}{2}} 2r \sin \frac{\alpha}{2} dx_1 + \int_{\frac{\pi}{2} + \frac{\theta}{2} - \frac{\alpha}{2}}^{\frac{5\pi}{2} - \frac{\theta}{2} - \frac{\alpha}{2}} r \sin \frac{\alpha}{2} + r \cos \left(x_1 - \frac{\theta}{2} \right) dx_1 + \int_{\frac{5\pi}{2} - \frac{\theta}{2} - \frac{\alpha}{2}}^{\frac{3\pi}{2}} 2r \sin \frac{\alpha}{2} dx_1 \right) \quad \text{eqn 1}$$

$$= \frac{r}{\pi} \left(\theta \sin \frac{\alpha}{2} - \cos \frac{\alpha}{2} + \cos \left(\frac{\alpha}{2} + \theta \right) \right) \quad \text{eqn 2}$$

217 We then use this expression to calculate density

$$218 \quad D = z/vt\bar{p}. \quad \text{eqn 3}$$

219 Rather than having one equation that describes \bar{p} globally, the gREM must be
 220 split into submodels due to discontinuous changes in p as α and β change. These
 221 discontinuities can occur for a number of reasons such as a profile switching be-
 222 tween being limited by α and θ , the difference between very small profiles and
 223 profiles of size zero, and the fact that the width of a sector stops increasing once
 224 the central angle reaches π radians (i.e., a semi-circle is just as wide as a full circle).
 225 As an example, if α is small, there is an interval between Figure 3c and 3d where
 226 the ‘blind spot’ would prevent animals being detected giving $p = 0$. This would
 227 require an extra integral in our equation, as simply putting our small value of α
 228 into eqn 1 would not give us this integral of $p = 0$.

229 gREM submodel specifications were done by hand, and the integration was
 230 done using SymPy (SymPy Development Team, 2014) in Python (Appendix S3).
 231 The gREM submodels were checked by confirming that: (1) submodels adjacent
 232 in parameter space were equal at the boundary between them; (2) submodels that
 233 border $\alpha = 0$ had $p = 0$ when $\alpha = 0$; (3) average profile widths \bar{p} were between 0
 234 and $2r$ and; (4) each integral, divided by the range of angles that it was integrated
 235 over, was between 0 and $2r$. The scripts for these tests are included in Appendix
 236 S3 and the R (Team, 2014) implementation of the gREM is given in Appendix S4.

237 **Simulation Model.** We tested the accuracy and precision of the gREM by devel-
 238 oping a spatially explicit simulation of the interaction of sensors and animals using
 239 different combinations of sensor detection widths, animal signal widths, number
 240 of captures, and models of animal movement. One hundred simulations were run

where each consisted of a 7.5 km by 7.5 km square with periodic boundaries. A stationary sensor of radius r , 10 m, was set up in the exact centre of each simulated study area, covering seven sensor detection widths θ , between 0 and 2π ($2/9\pi$, $4/9\pi$, $6/9\pi$, $8/9\pi$, $10/9\pi$, $14/9\pi$, and 2π). Each sensor was set to record continuously and to capture animal signals instantaneously from emission. Each simulation was populated with a density of 70 animals km^{-2} , calculated from the equation in Damuth (1981) as the expected density of mammals weighing 1 g. This density therefore represents a reasonable estimate of density of individuals, given that the smallest mammal is around 2 g (Jones *et al.*, 2009). A total of 3937 individuals per simulation were created which were placed randomly at the start of the simulation. 11 signal widths α between 0 and π were used ($1/11\pi$, $2/11\pi$, $3/11\pi$, $4/11\pi$, $5/11\pi$, $6/11\pi$, $7/11\pi$, $8/11\pi$, $9/11\pi$, $10/11\pi$, π).

Each simulation lasted for N steps (14400) of duration T (15 minutes) giving a total duration of 150 days. The individuals moved within each step with a distance d , with an average speed, v . The distance, d , was sampled from a normal distribution with mean distance, $\mu_d = vT$, and standard deviation, $\sigma_d = vT/10$, where the standard deviation was chosen to scale with the average distance travelled. An average speed, $v = 40 \text{ km day}^{-1}$, was chosen based on the largest day range of terrestrial animals (Carbone *et al.*, 2005), and represents the upper limit of realistic speeds. At the end of each step, individuals were allowed to either remain stationary for a time step (with a given probability, S), or change direction where the change in direction has a uniform distribution in the interval $[-A, A]$. This resulted in seven different movement models where: (1) simple movement, where S and $A = 0$; (2) stop-start movement, where (i) $S = 0.25$, $A = 0$, (ii) $S = 0.5$, $A = 0$, (iii) $S = 0.75$, $A = 0$; (3) correlated random walk movement, where (i) $S = 0$, $A = \pi/3$, (ii) $S = 0$, $A = 2\pi/3$, (iii) $S = 0$, $A = \pi$. Individuals were counted as they moved into the detection zone of the sensor per simulation.

We calculated the estimated animal density from the gREM by summing the number of captures per simulation and inputting these values into the correct gREM submodel. The accuracy of the gREM was determined by comparing the true simulation density with the estimated density. Precision of the gREM was determined by the standard deviation of estimated densities. We used this method to

compare the accuracy and precision of all the gREM submodels. As these submodels are derived for different combinations of α and θ , the accuracy and precision of the submodels was used to determine the impact of different values of α and θ .

The influence of the number of captures and animal movement models on accuracy and precision was investigated using four different gREM submodels representative of the range α and θ values (submodels NW1, SW1, NE1, and SE3, Figure 2). From a random starting point we ran the simulation until a range of different capture numbers were recorded (from 10 to 100 captures), recorded the length of time this took, and estimated the animal density for each of the four submodels. These estimated densities were compared to the true density to assess the impact on the accuracy and precision of the gREM. We calculated the coefficient of variation in order to compare the precision of the density estimates from simulations with different expected numbers of captures. The gREM also assumes that individuals move continuously with straight-line movement (simple movement model) and we therefore assessed the impact of breaking the gREM assumptions. We used the four submodels to compare the accuracy and precision of a simple movement model, stop-start movement models (using different average amounts of time spent stationary), and random walk movement models. Finally, as the parameters (α , β , r and v) are likely to be measured with error, we compared true simulation densities to densities estimated with parameters with errors of 0%, $\pm 5\%$ and $\pm 10\%$, for all gREM submodels.

RESULTS

Analytical model. The equation for \bar{p} has been newly derived for each submodel in the gREM, except for the gas model and REM which have been calculated previously. However, many models, although derived separately, have the same expression for \bar{p} . Figure 4 shows the expression for \bar{p} in each case. The general equation for density, eqn 3, is used with the correct value of \bar{p} substituted. Although more thorough checks are performed in Appendix S3, it can be seen that all adjacent expressions in Figure 4 are equal when expressions for the boundaries between them are substituted in.

Simulation model.

304 *gREM submodels.* All gREM submodels showed a high accuracy, i.e., the median
 305 difference between the estimated and true values was less than 2% across all mod-
 306 els (Figure 5). However, the precision of the submodels do vary, where the gas
 307 model is the most precise and the SW7 sub model the least precise, having the
 308 smallest and the largest interquartile range, respectively (Figure 5). The standard
 309 deviation of the error between the estimated and true densities is strongly related
 310 to both the sensor and signal widths (Appendix S5), such that larger widths have
 311 lower standard deviations (greater precision) due to the increased capture rate of
 312 these models.

313 *Number of captures.* Within the four gREM submodels tested (NW1, SW1, SE3,
 314 NE1), the accuracy was not strongly affected by the number of captures. The me-
 315 dian difference between the estimated and true values was less than 15% across
 316 all capture rates (Figure 6). However, the precision was dependent on the num-
 317 ber of captures across all four of the gREM submodels, where precision increases
 318 as number of captures increases, as would be expected for any statistical estimate
 319 (Figure 6). For all gREM submodels, the the coefficient of variation falls to 10% at
 320 100 captures.

321 *Movement models.* Within the four gREM submodels tested (NW1, SW1, SE3, NE1),
 322 neither the accuracy or precision was affected by the average amount of time spent
 323 stationary. The median difference between the estimated and true values was less
 324 than 2% for each category of stationary time (0, 0.25, 0.5 and 0.75) (Figure 7a).
 325 Altering the maximum change in direction in each step (0, $\pi/3$, $2\pi/3$, and π) did
 326 not affect the accuracy or precision of the four gREM submodels (Figure 7b).

327 *Impact of parameter error.* The percentage error in the density estimates across all
 328 parameters and gREM submodels shows a similar response for under and over
 329 estimated parameters, suggesting the accuracy is reasonable with respect to pa-
 330 rameter error (Appendix S6). The impact of parameter error on the precision of the
 331 density estimate varies across gREM submodels and parameters, where α shows
 332 the largest variation including the largest values. However, in all cases the per-
 333 centage error in the density estimate is not more than 5% greater than the error in
 334 the parameter estimate (Appendix S6).

DISCUSSION

Analytical model. We have developed the gREM such that it can be used to estimate density from acoustic sensors and camera traps. This has entailed a generalisation of the gas model and the REM in Rowcliffe *et al.* (2008) to be applicable to any combination of sensor width θ and signal directionality α . We emphasise that the approach is robust to multiple detections of the same individual. We have used simulations to show, as a proof of principle, that these models are accurate and precise.

There are a number of possible extensions to the gREM which could be developed in the future. The original gas model was formulated for the case where both animals and sensor are moving (Hutchinson & Waser, 2007). Indeed any of the models which have animals that are equally detectable in all directions ($\alpha = 2\pi$) can be trivially expanded by replacing animal speed v with $v + v_s$ where v_s is the speed of the sensor. However, when the animal has a directional call the extension becomes less simple. The approach would be to calculate again the mean profile width. However, for each angle of approach, one would have to average the profile width for an animal facing in any direction (i.e., not necessarily moving towards the sensor) weighted by the relative velocity of that direction. There are a number of situations where a moving detector and animal could occur, e.g. an acoustic detector towed from a boat when studying porpoises (Kimura *et al.*, 2014) or surveying echolocating bats from a moving car (Jones *et al.*, 2013).

Interesting but unstudied problems impacting the gREM are firstly, edge effects caused by sensor trigger delays (the delay between sensing an animal and attempting to record the encounter) (Rovero *et al.*, 2013), and secondly, sensors which repeatedly turn on and off during sampling (Jones *et al.*, 2013). The second problem is particularly relevant to acoustic detectors which record ultrasound by time expansion. Here ultrasound is recorded for a set time period and then slowed down and played back, rendering the sensor 'deaf' periodically during sampling. Both of these problems may cause biases in the gREM, as animals can move through the detection zone without being detected. As the gREM assumes constant surveillance, the error created by switching the sensor on and off quickly will become

more important if the sensor is only on for short periods of time. We recommend that the gREM is applied to constantly sampled data, and the impacts of breaking these assumptions on the gREM should be further explored.

Accuracy, Precision and Recommendations for Best Practice. Based on our simulations, we believe that the gREM has the potential to produce accurate estimates for many different species, using either camera traps or acoustic detectors. However, the precision of the gREM differed between submodels. For example, when the sensor and signal width were small, the precision of the model was reduced. Therefore when choosing a sensor for use in a gREM study, the sensor detection width should be maximised. If the study species has a narrow signal directionality, other aspects of the study protocol, such as length of the survey, should be used to compensate.

The precision of the gREM is greatly affected by the number of captures. The coefficient of variation falls dramatically between 10 and 60 captures and then after this continues to slowly reduce. At 100 captures the submodels reach 10% coefficient of variation, considered to be a very good level of precision and better than many previous studies (Thomas & Marques, 2012; O'Brien *et al.*, 2003; Foster & Harmsen, 2012). The length of surveys in the field will need to be adjusted so that enough data can be collected to reach this precision level. Populations of fast moving animals or populations with high densities will require less survey effort than those species that are slow moving or have populations with low densities.

We found that the sensitivity of the gREM to inaccurate parameter estimates was both predictable and reasonable (Appendix S6), although this varies between different parameters and gREM submodels. Whilst care should be taken in parameter estimation when analysing both acoustic and camera trap data, acoustic data poses particular problems. For acoustic surveys, estimates of r (detection distance) can be measured directly or calculated using sound attenuation models (Holderied & Von Helversen, 2003), while the sensor angle is often easily measured (Adams *et al.*, 2012) or found in the manufacturer's specifications. When estimating animal movement speed v , only the speed of movement during the survey period should be used. The signal width is the most sensitive parameter

397 to inaccurate estimates (Appendix S6) and is also the most difficult to measure.
 398 While this parameter will typically be assumed to be 2π for camera trap surveys,
 399 fewer estimates exist for acoustic signal widths. Although signal width has been
 400 measured for echolocating bats using arrays of microphones (Brinkløv *et al.*, 2011),
 401 more work should be done on obtaining estimates for a range of acoustically sur-
 402 veyed species.

403 **Limitations.** Although the REM has been found to be effective in field tests (Row-
 404 cliffe *et al.*, 2008; Zero *et al.*, 2013), the gREM requires further validation by both
 405 field tests and simulations. For example, capture-mark-recapture methods could
 406 be used alongside the gREM to test the accuracy under field conditions (Rowcliffe
 407 *et al.*, 2008). While we found no effect of the movement model on the accuracy
 408 or precision of the gREM, the models we have used in our simulations to vali-
 409 date the gREM are still simple representations of true animal movement. Animal
 410 movement may be highly nonlinear and often dependent on multiple factors such
 411 as behavioural state and existence of home ranges (Smouse *et al.*, 2010). There-
 412 fore testing the gREM against real animal data, or further simulations with more
 413 complex movement models, would be beneficial.

414 The assumptions of our simulations may require further consideration, for ex-
 415 ample we have assumed an equal density across the study area. However, in
 416 a field environment the situation may be more complex, with additional varia-
 417 tion coming from local changes in density between sensor sites. Although unequal
 418 densities should theoretically not affect accuracy (Hutchinson & Waser, 2007), it
 419 will affect precision and further simulations should be used to quantify this effect.
 420 Additionally, we allowed the sensor to be stationary and continuously detecting,
 421 negating the triggering, and non-continuous recording issues that could exist with
 422 some sensors and reduce precision or accuracy. Finally, in the simulation animals
 423 moved at the equivalent of the largest day range of terrestrial animals (Carbone
 424 *et al.*, 2005). Slower speed values should not alter the accuracy of the gREM, but
 425 precision would be affected since slower speeds produce fewer records. The gREM
 426 was both accurate and precise for all the movement models we tested (stop-start
 427 movement and correlated random walks).

A feature of the gREM is that it does not fit a statistical model to estimate detection probability as occupancy models and distance sampling do (Royle & Nichols, 2003; Barlow & Taylor, 2005; Marques *et al.*, 2011). Instead it explicitly models the process, with animals only being detected if they approach the sensor from a suitable direction. Other processes that affect detection probability could be included in the model to improve realism.

Implications for ecology and conservation. The gREM is applicable for count data obtained either visually or acoustically in both marine and terrestrial environments, and is suitable for taxa including echolocating bats (Walters *et al.*, 2012), songbirds (Buckland & Handel, 2006), whales (Marques *et al.*, 2011) and forest primates (Hassel-Finnegan *et al.*, 2008). Many of these taxa contain critically endangered species and monitoring their populations is of conservation interest. For example, current methods of density estimation for the threatened Franciscana dolphin (*Pontoporia blainvillei*) may result in underestimation of their numbers (Crespo *et al.*, 2010). In addition, using gREM may be easier than other methods for measuring the density of animals which may be useful in quantifying ecosystem services, such as songbirds with a known positive influence on pest control (Jirinec *et al.*, 2011).

The gREM will aid researchers to study species with non-invasive methods such as remote sensors, which allows for large, continuous monitoring projects with limited human resources (Kelly *et al.*, 2012). The gREM is also suitable for species that are sensitive to human contact or are difficult or dangerous to catch (Thomas & Marques, 2012). As sensors such as camera traps and acoustic detectors become more ubiquitous, the gREM will be increasingly useful for monitoring unmarked animal populations across broad spatial, temporal and taxonomic scales.

ACKNOWLEDGMENTS

We thank Hilde Wilkinson-Herbot, Chris Carbone, Francois Balloux, Andrew Cunningham, Steve Hailes, Richard Glennie and an anonymous referee for comments on previous versions of the manuscript. This study was funded through CoMPLEX PhD studentships at University College London supported by BBSRC

459 and EPSRC (EAM and TCDL); The Darwin Initiative (Awards 15003, 161333, EI-
460 DPR075 to KEJ), and The Leverhulme Trust (Philip Leverhulme Prize for KEJ).

461 REFERENCES

- 462 Acevedo, M.A. & Villanueva-Rivera, L.J. (2006) Using automated digital recording
463 systems as effective tools for the monitoring of birds and amphibians. *Wildlife*
464 *Society Bulletin*, **34**, 211–214.
- 465 Adams, A., Jantzen, M., Hamilton, R. & Fenton, M. (2012) Do you hear what I
466 hear? Implications of detector selection for acoustic monitoring of bats. *Methods*
467 *in Ecology and Evolution*.
- 468 Anderson, D.R. (2001) The need to get the basics right in wildlife field studies.
469 *Wildlife Society Bulletin*, **29**, 1294–1297.
- 470 Barlow, J. & Taylor, B. (2005) Estimates of sperm whale abundance in the north-
471 eastern temperate pacific from a combined acoustic and visual survey. *Marine*
472 *Mammal Science*, **21**, 429–445.
- 473 Blumstein, D.T., Mennill, D.J., Clemins, P., Girod, L., Yao, K., Patricelli, G., Deppe,
474 J.L., Krakauer, A.H., Clark, C., Cortopassi, K.A. *et al.* (2011) Acoustic monitoring
475 in terrestrial environments using microphone arrays: applications, technologi-
476 cal considerations and prospectus. *Journal of Applied Ecology*, **48**, 758–767.
- 477 Borchers, D., Distiller, G., Foster, R., Harmsen, B. & Milazzo, L. (2014) Continuous-
478 time spatially explicit capture–recapture models, with an application to a jaguar
479 camera-trap survey. *Methods in Ecology and Evolution*, **5**, 656–665.
- 480 Brinkløv, S., Jakobsen, L., Ratcliffe, J., Kalko, E. & Surlykke, A. (2011) Echoloca-
481 tion call intensity and directionality in flying short-tailed fruit bats, *Carollia per-*
482 *spicillata* (phyllostomidae). *The Journal of the Acoustical Society of America*, **129**,
483 427–435.
- 484 Brusa, A. & Bunker, D.E. (2014) Increasing the precision of canopy closure es-
485 timates from hemispherical photography: Blue channel analysis and under-
486 exposure. *Agricultural and Forest Meteorology*, **195**, 102–107.
- 487 Buckland, S.T. & Handel, C. (2006) Point-transect surveys for songbirds: robust
488 methodologies. *The Auk*, **123**, 345–357.

- 489 Buckland, S.T., Marsden, S.J. & Green, R.E. (2008) Estimating bird abundance:
490 making methods work. *Bird Conservation International*, **18**, S91–S108.
- 491 Carbone, C., Cowlishaw, G., Isaac, N.J. & Rowcliffe, J.M. (2005) How far do ani-
492 mals go? Determinants of day range in mammals. *The American Naturalist*, **165**,
493 290–297.
- 494 Crespo, E.A., Pedraza, S.N., Grandi, M.F., Dans, S.L. & Garaffo, G.V. (2010) Abun-
495 dance and distribution of endangered Franciscana dolphins in Argentine waters
496 and conservation implications. *Marine Mammal Science*, **26**, 17–35.
- 497 Damuth, J. (1981) Population density and body size in mammals. *Nature*, **290**,
498 699–700.
- 499 Depraetere, M., Pavoine, S., Jiguet, F., Gasc, A., Duvail, S. & Sueur, J. (2012) Mon-
500 itoring animal diversity using acoustic indices: implementation in a temperate
501 woodland. *Ecological Indicators*, **13**, 46–54.
- 502 Everatt, K.T., Andresen, L. & Somers, M.J. (2014) Trophic scaling and occupancy
503 analysis reveals a lion population limited by top-down anthropogenic pressure
504 in the Limpopo National Park, Mozambique. *PloS one*, **9**, e99389.
- 505 Foster, R.J. & Harmsen, B.J. (2012) A critique of density estimation from camera-
506 trap data. *The Journal of Wildlife Management*, **76**, 224–236.
- 507 Harris, D., Matias, L., Thomas, L., Harwood, J. & Geissler, W.H. (2013) Applying
508 distance sampling to fin whale calls recorded by single seismic instruments in
509 the northeast Atlantic. *The Journal of the Acoustical Society of America*, **134**, 3522–
510 3535.
- 511 Hassel-Finnegan, H.M., Borries, C., Larney, E., Umponjan, M. & Koenig, A. (2008)
512 How reliable are density estimates for diurnal primates? *International Journal of*
513 *Primateology*, **29**, 1175–1187.
- 514 Holderied, M. & Von Helversen, O. (2003) Echolocation range and wingbeat pe-
515 riod match in aerial-hawking bats. *Proc R Soc B*, **270**, 2293–2299.
- 516 Hutchinson, J.M.C. & Waser, P.M. (2007) Use, misuse and extensions of “ideal gas”
517 models of animal encounter. *Biological Reviews of the Cambridge Philosophical So-*
518 *ciety*, **82**, 335–359.
- 519 Jirinec, V., Campos, B.R. & Johnson, M.D. (2011) Roosting behaviour of a migratory
520 songbird on Jamaican coffee farms: landscape composition may affect delivery

- of an ecosystem service. *Bird Conservation International*, **21**, 353–361.
- Jones, K.E., Bielby, J., Cardillo, M., Fritz, S.A., O'Dell, J., Orme, C.D.L., Safi, K., Sechrest, W., Boakes, E.H., Carbone, C., Connolly, C., Cutts, M.J., Foster, J.K., Grenyer, R., Habib, M., Plaster, C.A., Price, S.A., Rigby, E.A., Rist, J., Teacher, A., Bininda-Emonds, O.R.P., Gittleman, J.L., Mace, G.M., Purvis, A. & Michener, W.K. (2009) PanTHERIA: a species-level database of life history, ecology, and geography of extant and recently extinct mammals. *Ecology*, **90**, 2648.
- Jones, K.E., Russ, J.A., Bashta, A.T., Bilhari, Z., Catto, C., Csősz, I., Gorbachev, A., Győrfi, P., Hughes, A., Ivashkiv, I., Koryagina, N., Kurali, A., Langton, S., Collen, A., Margiean, G., Pandourski, I., Parsons, S., Prokofev, I., Szodoray-Paradi, A., Szodoray-Paradi, F., Tilova, E., Walters, C.L., Weatherill, A. & Zavarzin, O. (2013) Indicator bats program: A system for the global acoustic monitoring of bats. B. Collen, N. Pettorelli, J.E.M. Baillie & S.M. Durant, eds., *Biodiversity Monitoring and Conservation*, pp. 211–247. Wiley-Blackwell.
- Karanth, K. (1995) Estimating tiger (*Panthera tigris*) populations from camera-trap data using capture–recapture models. *Biological Conservation*, **71**, 333–338.
- Kelly, M.J., Betsch, J., Wultsch, C., Mesa, B. & Mills, L.S. (2012) Noninvasive sampling for carnivores. L. Boitani & R. Powell, eds., *Carnivore ecology and conservation: a handbook of techniques*, pp. 47–69. Oxford University Press, New York.
- Kessel, S., Cooke, S., Heupel, M., Hussey, N., Simpfendorfer, C., Vagle, S. & Fisk, A. (2014) A review of detection range testing in aquatic passive acoustic telemetry studies. *Reviews in Fish Biology and Fisheries*, **24**, 199–218.
- Kimura, S., Akamatsu, T., Dong, L., Wang, K., Wang, D., Shibata, Y. & Arai, N. (2014) Acoustic capture-recapture method for towed acoustic surveys of echolocating porpoises. *The Journal of the Acoustical Society of America*, **135**, 3364–3370.
- Lewis, T., Gillespie, D., Lacey, C., Matthews, J., Danbolt, M., Leaper, R., McLanaghan, R. & Moscrop, A. (2007) Sperm whale abundance estimates from acoustic surveys of the Ionian Sea and Straits of Sicily in 2003. *Journal of the Marine Biological Association of the United Kingdom*, **87**, 353–357.
- MacKenzie, D.I. & Royle, J.A. (2005) Designing occupancy studies: general advice and allocating survey effort. *Journal of Applied Ecology*, **42**, 1105–1114.

- 552 Marcoux, M., Auger-Méthé, M., Chmelnitsky, E.G., Ferguson, S.H. & Humphries,
553 M.M. (2011) Local passive acoustic monitoring of narwhal presence in the Cana-
554 dian Arctic: a pilot project. *Arctic*, **64**, 307–316.
- 555 Marques, T.A., Munger, L., Thomas, L., Wiggins, S. & Hildebrand, J.A. (2011) Es-
556 timating North Pacific right whale (*Eubalaena japonica*) density using passive
557 acoustic cue counting. *Endangered Species Research*, **13**, 163–172.
- 558 Marques, T.A., Thomas, L., Martin, S.W., Mellinger, D.K., Ward, J.A., Moretti, D.J.,
559 Harris, D. & Tyack, P.L. (2013) Estimating animal population density using pas-
560 sive acoustics. *Biological Reviews*, **88**, 287–309.
- 561 O’Brien, T.G., Kinnaird, M.F. & Wibisono, H.T. (2003) Crouching tigers, hidden
562 prey: Sumatran tiger and prey populations in a tropical forest landscape. *Animal*
563 *Conservation*, **6**, 131–139.
- 564 Purvis, A., Gittleman, J.L., Cowlshaw, G. & Mace, G.M. (2000) Predicting extinc-
565 tion risk in declining species. *Proceedings of the Royal Society of London Series B:*
566 *Biological Sciences*, **267**, 1947–1952.
- 567 Rogers, T.L., Ciaglia, M.B., Klinck, H. & Southwell, C. (2013) Density can be mis-
568 leading for low-density species: benefits of passive acoustic monitoring. *Public*
569 *Library of Science One*, **8**, e52542.
- 570 Rovero, F., Zimmermann, F., Berzi, D. & Meek, P. (2013) “Which camera trap type
571 and how many do I need?” a review of camera features and study designs for a
572 range of wildlife research applications. *Hystrix*, **24**, 148–156.
- 573 Rowcliffe, J.M. & Carbone, C. (2008) Surveys using camera traps: are we looking
574 to a brighter future? *Animal Conservation*, **11**, 185–186.
- 575 Rowcliffe, J., Field, J., Turvey, S. & Carbone, C. (2008) Estimating animal density
576 using camera traps without the need for individual recognition. *Journal of Ap-*
577 *plied Ecology*, **45**, 1228–1236.
- 578 Royle, J.A. & Nichols, J.D. (2003) Estimating abundance from repeated presence-
579 absence data or point counts. *Ecology*, **84**, 777–790.
- 580 Schmidt, B.R. (2003) Count data, detection probabilities, and the demography, dy-
581 namics, distribution, and decline of amphibians. *Comptes Rendus Biologies*, **326**,
582 119–124.

- 583 Smouse, P.E., Focardi, S., Moorcroft, P.R., Kie, J.G., Forester, J.D. & Morales, J.M.
584 (2010) Stochastic modelling of animal movement. *Philosophical Transactions of the*
585 *Royal Society B: Biological Sciences*, **365**, 2201–2211.
- 586 SymPy Development Team (2014) *SymPy: Python library for symbolic mathematics*.
587 Team, R.C. (2014) *R: A Language and Environment for Statistical Computing*. R Foun-
588 dation for Statistical Computing, Vienna, Austria.
- 589 Thomas, L. & Marques, T.A. (2012) Passive acoustic monitoring for estimating an-
590 imal density. *Acoustics Today*, **8**, 35–44.
- 591 Walters, C.L., Collen, A., Lucas, T., Mroz, K., Sayer, C.A. & Jones, K.E. (2013) Chal-
592 lenges of using bioacoustics to globally monitor bats. R.A. Adams & S.C. Ped-
593 ersen, eds., *Bat Evolution, Ecology, and Conservation*, pp. 479–499. Springer.
- 594 Walters, C.L., Freeman, R., Collen, A., Dietz, C., Brock Fenton, M., Jones, G., Obrist,
595 M.K., Puechmaille, S.J., Sattler, T., Siemers, B.M. *et al.* (2012) A continental-scale
596 tool for acoustic identification of European bats. *Journal of Applied Ecology*, **49**,
597 1064–1074.
- 598 Wright, S.J. & Hubbell, S.P. (1983) Stochastic extinction and reserve size: a focal
599 species approach. *Oikos*, pp. 466–476.
- 600 Yapp, W. (1956) The theory of line transects. *Bird Study*, **3**, 93–104.
- 601 Zero, V.H., Sundaesan, S.R., O'Brien, T.G. & Kinnaird, M.F. (2013) Monitoring
602 an endangered savannah ungulate, Grevy's zebra (*Equus grevyi*): choosing a
603 method for estimating population densities. *Oryx*, **47**, 410–419.

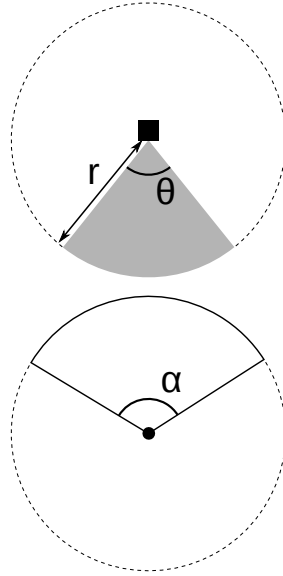


Figure 1. Representation of sensor detection width and animal signal width. The filled square and circle represent a sensor and an animal, respectively; θ , sensor detection width (radians); r , sensor detection distance; dark grey shaded area, sensor detection zone; α , animal signal width (radians). Dashed lines around the filled square and circle represents the maximum extent of θ and α , respectively.

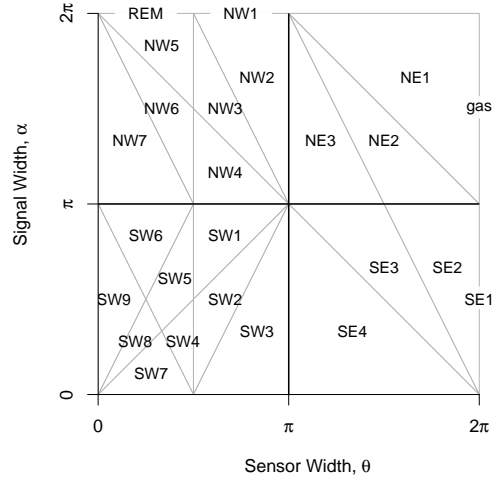


Figure 2. Locations where derivation of the average profile \bar{p} is the same for different combinations of sensor detection and animal signal widths. Symbols within each polygon refer to each gREM submodel named after their compass point, except for Gas and REM which highlight the position of these previously derived models within the gREM. Symbols on the edge of the plot are for submodels where $\alpha, \theta = 2\pi$

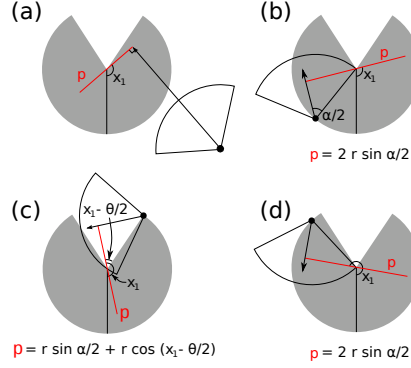


Figure 3. An overview of the derivation of the average profile \bar{p} for the gREM submodel SE2, where (a) shows the location of the profile p (the line an animal must pass through in order to be captured) in red and the focal angle, x_1 , for an animal (filled circle), its signal (unfilled sector), and direction of movement (shown as an arrow). The detection zone of the sensor is shown as a filled grey sector with a detection distance of r . The vertical black line within the circle shows the direction the sensor is facing. The derivation of p changes as the animal approaches the sensor from different directions (shown in b-d), where (b) is the derivation of p when x_1 is in the interval $[\frac{\pi}{2}, \frac{\pi}{2} + \frac{\theta}{2} - \frac{\alpha}{2}]$, (c) p when x_1 is in the interval $[\frac{\pi}{2} + \frac{\theta}{2} - \frac{\alpha}{2}, \frac{5\pi}{2} - \frac{\theta}{2} - \frac{\alpha}{2}]$ and (d) p when x_1 is in the interval $[\frac{5\pi}{2} - \frac{\theta}{2} - \frac{\alpha}{2}, \frac{3\pi}{2}]$, where θ , sensor detection width; α , animal signal width. The resultant equation for p is shown beneath b-d. The average profile \bar{p} is the size of the profile averaged across all approach angles.

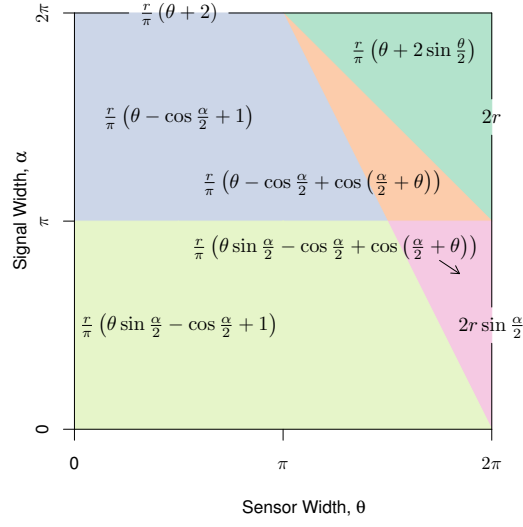


Figure 4. Expressions for the average profile width, \bar{p} , given a range of sensor and signal widths. Despite independent derivation within each block, many models result in the same expression. These are collected together and presented as one block of colour. Expressions on the edge of the plot are for submodels with $\alpha, \theta = 2\pi$.

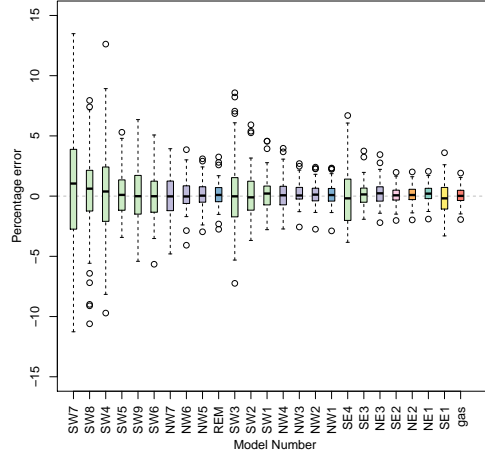


Figure 5. Simulation model results of the accuracy and precision for gREM submodels. The percentage error between estimated and true density for each gREM sub model is shown within each box plot, where the black line represents the median percentage error across all simulations, boxes represent the middle 50% of the data, whiskers represent variability outside the upper and lower quartiles with outliers plotted as individual points. Box colours correspond to the expressions for average profile width \bar{p} given in Figure 4.

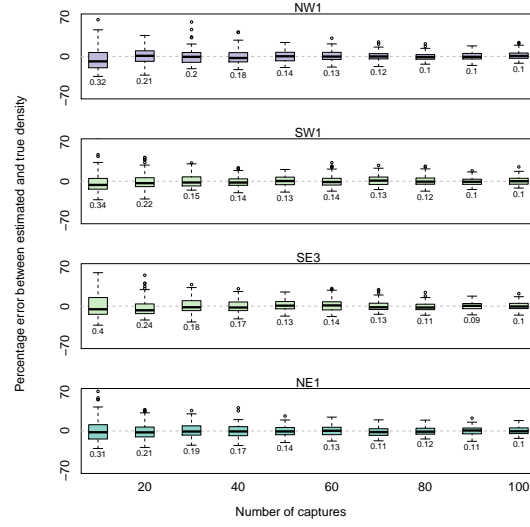


Figure 6. Simulation model results of the accuracy and precision of four gREM submodels (NW1, SW1, SE3 and NE1) given different numbers of captures. The percentage error between estimated and true density within each gREM sub model for capture rate is shown within each box plot, where the black line represents the median percentage error across all simulations, boxes represent the middle 50% of the data, whiskers represent variability outside the upper and lower quartiles with outliers plotted as individual points. Sensor and signal widths vary between submodels. The numbers beneath each plot represent the coefficient of variation. The colour of each box plot corresponds to the expressions for average profile width \bar{p} given in Figure 4.

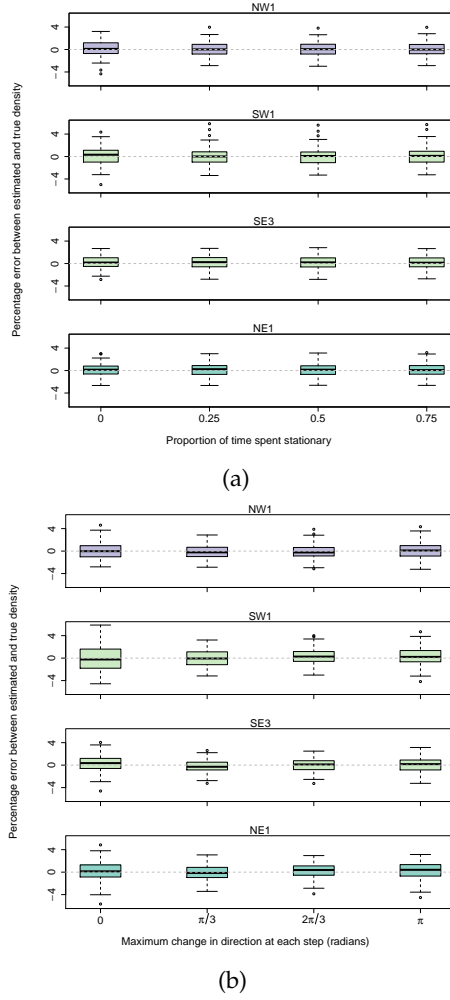


Figure 7. Simulation model results of the accuracy and precision of four gREM submodels (NW1, SW1, SE3 and NE1) given different movement models where (a) average amount of time spent stationary (stop-start movement) and (b) maximum change in direction at each step (correlated random walk model). The percentage error between estimated and true density within each gREM sub model for the different movement models is shown within each box plot, where the black line represents the median percentage error across all simulations, boxes represent the middle 50% of the data, whiskers represent variability outside the upper and lower quartiles with outliers plotted as individual points. The simple model is represented where time and maximum change in direction equals 0. The colour of each box plot corresponds to the expressions for average profile width \bar{p} given in Figure 4.